JOURNAL OF MATERIALS SCIENCE **36** (2001) 4643–4648

Electrical and thermal conductivity of A319 and A356 aluminum alloys

S. I. BAKHTIYAROV, R. A. OVERFELT, S. G. TEODORESCU
Department of Mechanical Engineering, 201 Ross Hall, Auburn University, AL 36849-5341, USA

A rotational contactless inductive measurement technique has been used to measure the electrical resistivity of A319 and A356 aluminum alloys at both solid and liquid states. The method is based on the phenomena that when a conducting material rotates in a magnetic field, circulating eddy currents are induced and generate an opposing torque, which is proportional to the electrical conductivity of the material. The technique was checked and calibrated with pure aluminum where considerable electrical resistivity data exist in the literature. Wiedemann-Franz-Lorenz law was used to estimate the thermal conductivity of A319 and A356 aluminum alloys in liquid state. © *2001 Kluwer Academic Publishers*

1. Introduction

Dependable information of various thermophysical properties (i.e., viscosity, electrical resistivity, density, thermal conductivity, etc.) of liquid metals can be of great significance to produce high-quality ingot and shaped casting components. Optimization and control of the metallurgical processes require accurate and precise materials data.

Information on the electrical resistivity of molten alloys is especially important in many metallurgical processes such as electroslug remelting, electromagnetic stirring in continuous casting, and induction melting in foundries. Due to their disordered arrangement of ions in the liquid state, molten metals exhibit higher electrical resistivity than solid metals (∼1.5–2.3 times higher). However, relatively few studies have been reported on the electrical resistivity (or conductivity) of molten metals and alloys, particularly at elevated temperatures, since the measurements are extremely difficult. The methods of electrical resistivity measurements can be categorized into two groups:

- direct resistance measurements using contact probes and
- contactless inductive measurements.

The technique of choice for solid materials is the direct resistance four-probe method [1–3] which is based upon application of Ohm's law. Although this direct method can be applied to low melting point, non-reactive liquid materials, reactions between the probes and the molten sample preclude using the four-probe method with high-melting point materials. In this method, the voltage drop along a sample in a capillary tube of known cross-section and length is measured at a constant current density. The probe cell has to be calibrated using a liquid metal (usually mercury) of known resistivity. Selection of the proper materials for the capillary cell and the electrodes remains the primary difficulty with this method. An improved four-probe method utilizing solid electrodes made of material which is identical to the molten sample has been reported [4]. However, this technique is limited to materials with very narrow freezing ranges.

Inductive techniques for measuring electrical resistivity are contactless and thus prevent chemical reactions between molten samples and contacting probes as in the direct method. When applied to molten metals, the method is usually based on the phenomena that when a metal sample rotates in a magnetic field (or the magnetic field rotates around a stationary sample), circulating eddy currents are induced in the sample which generate an opposing torque proportional to the electrical conductivity of the sample [1]. In liquid metals and alloys the applied magnetic field also causes significant rotation of the liquid in the crucible which decreases the angular velocity between the field and the sample [5]. Recently, Bakhtiyarov and Overfelt [28, 29] developed a rotational contactless inductive measurement technique to measure the both viscosity and the electrical conductivity of liquid metals. Preliminary tests conducted with low melting point metals (lead and tin) and alloys (LMA-158 and Pb/Sn binary systems) showed a good agreement with data from the literature. This technique requires a reliable relationship between the electrical resistivity of the metal sample and the measured damping torque values. Braunbeck [6] proposed the following relationship between the opposing mechanical torque (T) and the electric conductivity of a rotating liquid specimen (σ_e) in a DC external magnetic field of induction B:

$$T = \frac{\pi}{4}\sigma_e \omega L R^4 B^2 - \frac{\pi}{192}\frac{1}{\eta}\sigma_e^2 \omega L R^6 B^4, \qquad (1)$$

where L and R are length and radius of the specimen, respectively; ω is the angular velocity of the rotating magnetic field; and η is the viscosity of the liquid specimen.

The magnetic induction and the radius of the specimen can be selected so that the second term in Equation 1 will become negligibly small compared with the first term for measurements on metals with unknown viscosity [7].

Spitzer *et al*. [8] studied electromagnetic stirring in continuous casting of round strands. A finite difference model was developed for the computation of the flow field in continuous casting through the simultaneous solution of the Navier-Stokes equations, the continuity equation, and the Maxwell equation. These authors also presented a simplified analytical model for an infinitely long cylinder. In addition, experimental data on the rotation of liquid mercury in plexiglass cylinder subject to a rotating magnetic field was shown for comparison. Spitzer *et al*. [8] found that the wall shear stresses from the numerical model and the analytical model agreed very well with the experimental data for liquid mercury. This indicated that the flow field in the vicinity of the plexiglass wall was predicted correctly. Thus from Spitzer *et al*. [8]

$$\tau_w = \frac{1}{8}\sigma_e \omega R^3 B^2. \tag{2}$$

(Note that the superscript of R should be 3 instead of 2 as in Reference 8.) However, Spitzer *et al*. [8] correctly point out that more complex convection effects in the interior of the samples could not be adequately predicted from the simple analytical theory and resolution of these effects required use of the numerical model. Since the wetted area is $L(2\pi R)$, the torque per unit length exerted on the crucible from the magnetic interaction should be

$$\frac{T}{L} = \frac{\pi}{4}\sigma_e \omega R^4 B^2. \tag{3}$$

Equation 3 is the same as the first term in Equation 1 from Braunbeck [6].

Electromagnetic levitation is another technique for containerless measurements of electrical conductivity in liquid metals. It combines the containerless positioning method of electromagnetic levitation with the contactless technique of inductive electrical conductivity measurement. Until now this technique has been applied only to low melting point metals contained in an ampoules to give the material a cylindrical shape. The sample without container will be freely suspended within the measuring field and will have no predefined shape. Currently, there are two main problems with usage of this technique, which has to be solved.

First, it is impossible to define exact location and shape of the sample. Second, there is a mutual inductive interaction between the levitation and the measurement circuits.

The objective of this paper is to present the electrical conductivity data for pure aluminum, A319 and A356 aluminum alloys obtained by direct measurements on rotational technique (with a cylindrical metal sample rotating in a 2-pole DC magnetic field) over wide ranges of temperatures. An indirect determination of the thermal conductivity through the Wiedemann-Franz-Lorenz law was performed for test specimen.

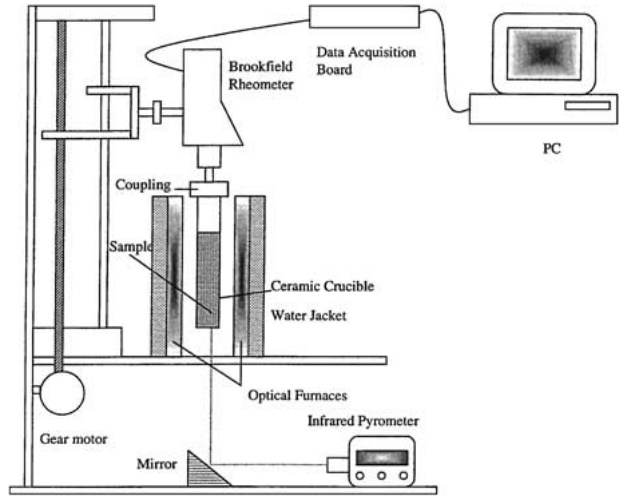

Figure 1 Experimental apparatus used for electrical resistivity measurements of solid and molten metals.

2. Experimental apparatus and procedures

A schematic of the experimental apparatus to measure an electrical resistivity of metals and alloys at high temperatures is shown in Fig. 1. A computer controlled Brookfield rheometer Model DV-III was used to provide a constant rotational speed to the metal sample and to measure the torque. This rheometer enables torque measurements from 0 to 673.7 dyne-cm at constant speeds from 0 to 250 RPM in 0.1 RPM increments. The rheometer has an RS232 serial port for communication with a local computer.

The temperature of the samples were characterized remotely by an portable 2-color infrared thermometer M90 (Mikron®) focused into a hole in the bottom of the crucible assembly since thermocouple leads could not be inserted into the rotating samples. Focusing into the hole in the crucible bottom eliminated spurious temperature data from extraneous reflections into the infrared thermometer from the optical heaters. The infrared thermometer output was calibrated to actual temperature by comparing against thermocouple data using a dummy load with 0.25% accuracy. The thermometer output was connected to computer and the temperature data obtained were synchronized with data for measured torque and angular velocity of the crucible.

Metal samples (9.525 to 19.05 mm diameter and 25.4 to 38.1 mm length) for testing were inserted into cylindrical high purity alumina crucibles with flat bottom. The extruded alumina crucibles (19.05 mm inner diameter and 152.4 mm length) were attached to the spindle of the rheometer through a specially designed coupler to provide concentricity to the rotating shaft, crucible and sample. The same sample diameter was maintained for each set of tests. The rotational technique of this geometry is exposed to the end effects in the crucible. The effect was eliminated from the results of two experiments accomplished with the different heights (25.4 mm and 38.1 mm) of the liquid in the annular space between the cylinders but at the same angular speed.

Two quartz infrared line heating elements (2 kW each) housed in elliptical cast aluminum frames were used to heat the samples in the experiments. The heated length of the chamber was 167 mm. The elliptical

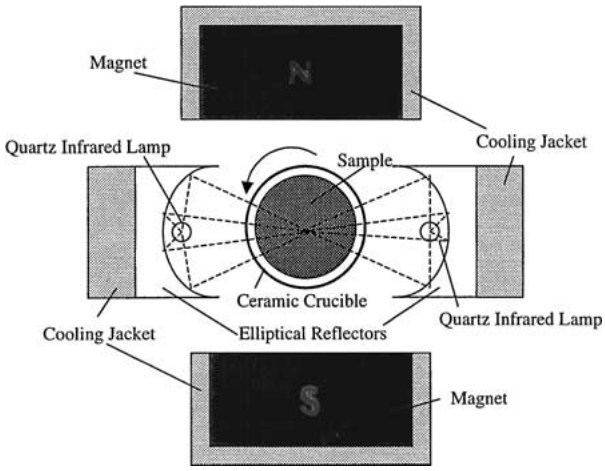

Figure 2 Diagram of sample-magnetic field-optical furnace arrangement and heating energy focus action.

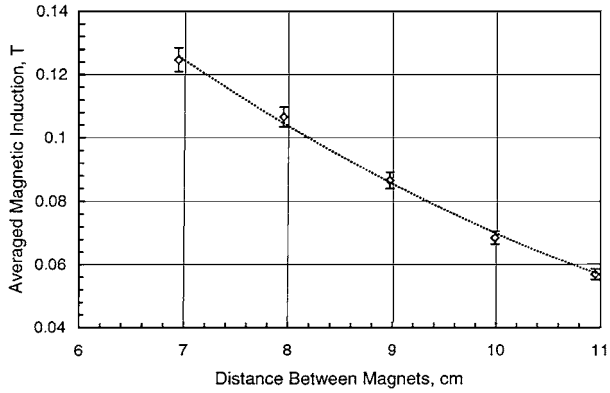

Figure 3 Variation of averaged magnetic induction with distance between magnets.

reflectors concentrated the infrared energy to the crucible surface (Fig. 2). Copper tube connections are provided for inlet and outlet flow of water to cool the lamp reflector bodies. Tap water at 15°C and 600 kPa was supplied to cool the unit.

The magnetic field was produced by two neodymium-iron permanent magnets. A Hall-effect gaussmeter was used to measure the magnetic field strength. The gaussmeter provides DC and AC field readings from $\pm 10^{-5}$ to ± 2 Tesla with 0.1% resolution. Changing the separation between the magnets allowed us to obtain magnetic fields of different magnitudes. Fig. 3 shows the variation of the magnetic induction with the distance between the magnets. Contour mapping of the magnetic field strength revealed that the magnetic induction varies in both vertical and horizontal directions. Contour lines for the magnetic induction at different distances between the magnets are shown in Fig. 4. It is estimated that the magnetic induction over the test sample varies $\pm 10\%$ in vertical direction and $\pm 7\%$ in horizontal direction compared to its average value. Neither the coupling system nor the alumina crucible had measurable effects upon the applied magnetic field.

As test sample we used pure aluminum (99.999% purity), A319 and A356 aluminum alloys. The composition and some thermophysical properties of A319 and A356 aluminum alloys are given in Table I. The electrical resistances of solid samples were measured with 4300B Digital Micro-ohmmeter from Valhalla Scientific, Inc. to provide independent data on the electrical resistivity of solid samples for comparison. The Kelvin four-terminal configuration of this ohmmeter eliminates errors caused by test lead and contact resistance, which in many applications can exceed the value of the load, by several orders of magnitude.

TABLE I Thermophysical properties and composition of A319 and A356 aluminum alloys [30]

A319 aluminum alloy		A356 aluminum alloy	
Solidus temperature	723 K	Solidus temperature	831 K
Liquidus temperature	869 K	Liquidus temperature	876 K
Latent heat	400 J/g	Latent heat	429 J/g
Density at melting point	2.5328 g/cm^3	Density at melting point	2.362 g/cm^3
Composition	Si = 6.1%	Composition	Si = 6.9%
	Fe = 0.68%		Fe = 0.08%
	Mg = 0.3%		Mg = 0.34%
	Cu = 3.01%		Ti = 0.013%
	Mn = 0.32%		B = 0%
	Zn = 0.71%		Sr = 0%

3. Results and discussion

From both scientific and practical point of view, it is meaningful to know the order of the Reynolds number

$$\mathrm{Re} = VL\rho/\eta \tag{4}$$

and the *magnetic* Reynolds number ($\mathrm{Re_m}$) defined as [5]

$$\mathrm{Re}_m = 4\pi\mu\sigma_e LV, \tag{5}$$

where V and L are the characteristic velocity and length, respectively, ρ is the density, and the other parameters are as defined above. For this flow geometry, R is a convenient characteristic length, and the velocity can be taken as ωR. For the nonmagnetic materials under investigation here, μ can be taken as μ_o, the magnetic permeability of free space (1.2566×10^{-6} Vs A^{-1} m^{-1}). Substituting $V = \omega R$, $L = R$ and $\mu = \mu_o$ in Equations 4 and 5 gives

$$\mathrm{Re} = \omega R^2\rho/\eta \tag{6}$$

and

$$\mathrm{Re_m} = 4\pi\omega\mu_0\sigma_e R^2. \tag{7}$$

Figs 5 and 6 show the variation of Re and Re_m, respectively, with the angular velocity for the test samples investigated in these experiments. As seen from Fig. 5, $Re < 10^3$, which means the laminar flow conditions were maintained in these experiments. As seen from Fig. 6, $Re_\mathrm{m} \ll 1$. This has the practical significance that the magnetic field distribution is not affected by fluid motion and may be evaluated as though the conducting fluid were a solid [5]. Such a problem is a linear problem of well-known type [17, 18].

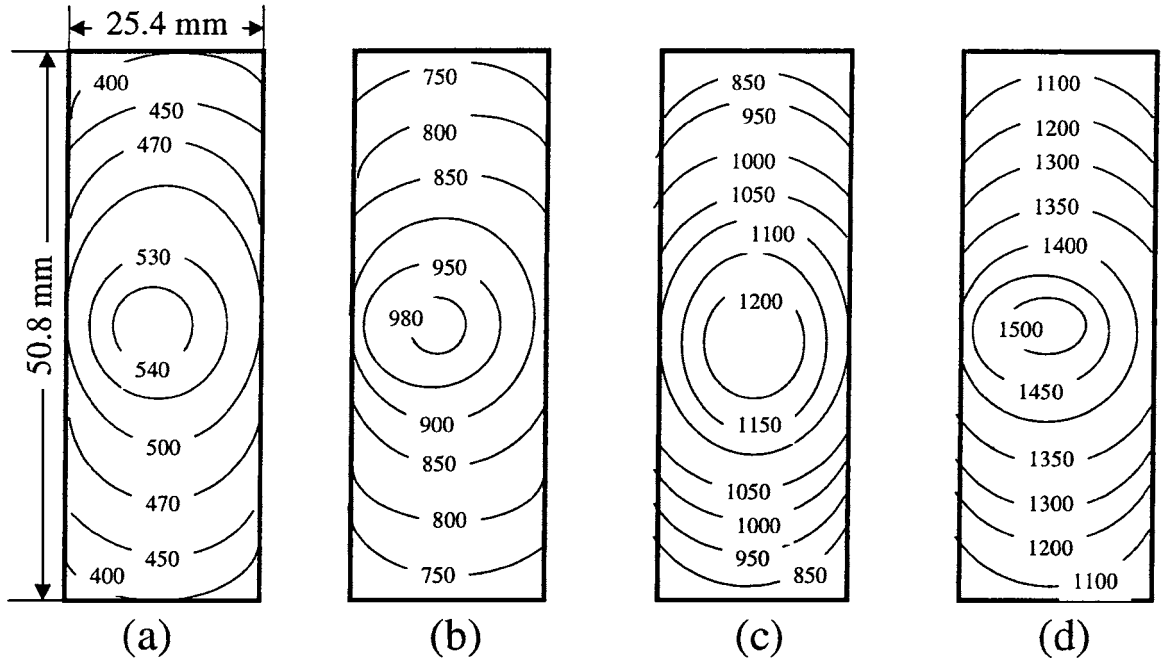

Figure 4 Contour lines for magnetic induction (in 10^{-4} T) at different distances between magnets: (a) 12 cm; (b) 9 cm; (c) 8 cm; (d) 7 cm.

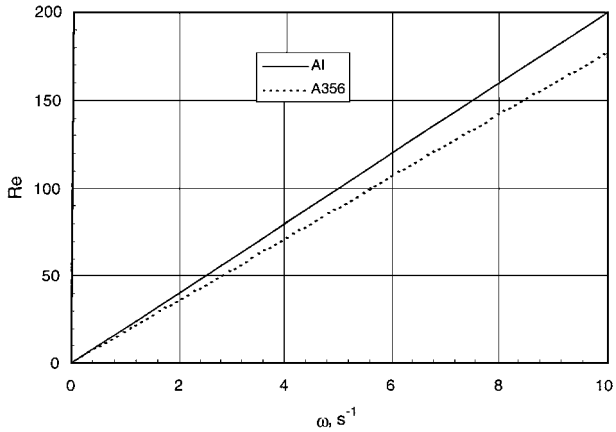

Figure 5 Variation of the Reynolds number with the angular velocity for liquid aluminum and A356 alloy samples. Calculated with Equation 6.

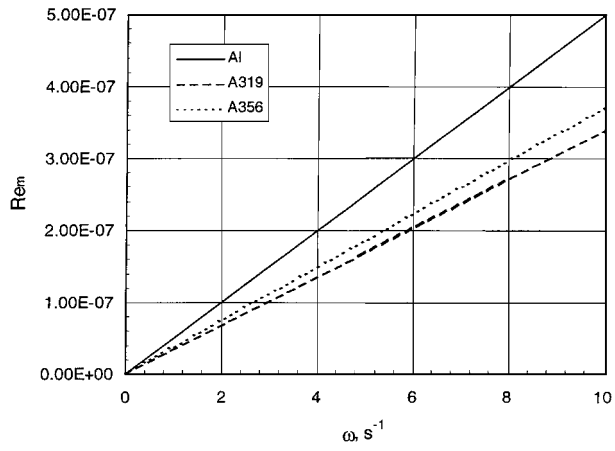

Figure 6 Variation of the magnetic Reynolds number with the angular velocity for liquid aluminum, A319 and A356 alloys samples. Calculated with Equation 7.

The variation of the eddy-current induced damping torques for pure aluminum, A319 and A356 aluminum alloy samples, with the temperature at $\omega = 3.66$ s^{-1} is shown in Fig. 7. As seen from these data, damping

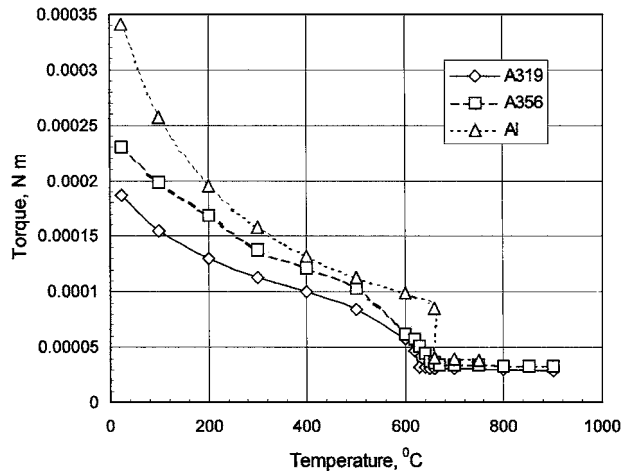

Figure 7 Variation of damping torque with temperature for pure aluminum, A319 amd A356 aluminum alloys.

torque decreases linearly with temperature for samples at solid state. A sudden decrease in damping torque occurs at melting points. Increasing the temperature does not change significantly the damping torque in liquid samples. Estimates of the magnitude of the second term in Equation 1 indicated that it was negligibly small (0.05–0.15%) compared with the first term for all test samples and thus Equation 3 should represent the data well. Excellent agreement between the experimental data and the theoretical calculations was found for the liquid aluminum samples.

The temperature dependence of the electrical resistivity of pure aluminum, A319 and A356 aluminum alloys is shown in Fig. 8. As seen from this figure, the measured values of the electrical resistivity for all samples are linearly related to the temperature over wide ranges of temperature below and above their melting points. There is a good agreement between the present data and data obtained previously by different researchers for pure aluminum. Fig. 9 represents

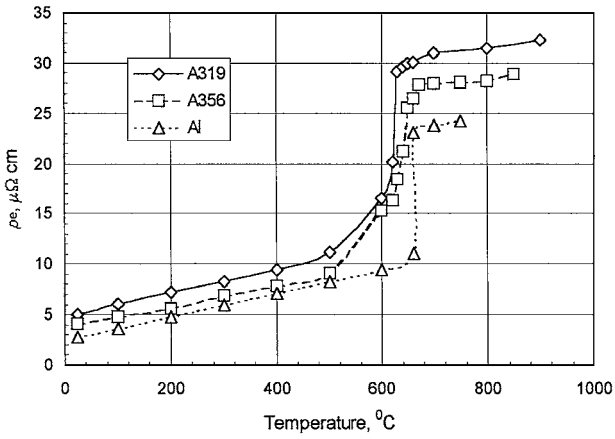

Figure 8 Variation of electrical resistivity with temperature for pure aluminum, A319 and A356 aluminum alloys.

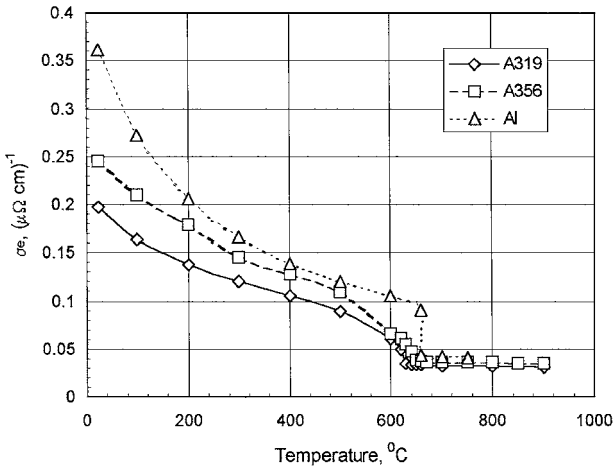

Figure 9 Variation of electrical conductivity with temperature for pure aluminum, A319 and A356 aluminum alloys.

the variation of the electrical conductivity (reciprocal of the electrical resistivity) with the temperature.

The electrical resistivity of liquid metals increases linearly with increasing temperature (except for Cd and Zn) [1]. This relationship can be expressed as

$$\rho_e = \alpha T + \beta, \tag{8}$$

where α and β are temperature coefficients of the electrical resistivity for liquid metals. According to Cusak and Enderby [22], over the temperature range from the melting point to 1473 K, temperature coefficients of the electrical resistivity for liquid aluminum are $\alpha = 0.0145\ \mu\Omega\,\mathrm{cm\,K^{-1}}$ and $\beta = 10.7\ \mu\Omega\,\mathrm{cm}$. The measured values of α and β for molten aluminum samples at different temperatures are presented in Fig. 10. The lines denote the values proposed by Cusak and Enderby [22]. Good agreement is exhibited between the values measured in the present investigation and the earlier literature values [22].

Free electrons are responsible for the electrical and thermal conductivities of metals and alloys in both solid and liquid states. Therefore, the Wiedemann-Franz-Lorenz law can be applied to relate the thermal conductivity to the electrical resistivity:

$$\frac{\lambda \rho_e}{T} = \frac{\pi \kappa^2}{3e^2} \equiv L_0, \tag{9}$$

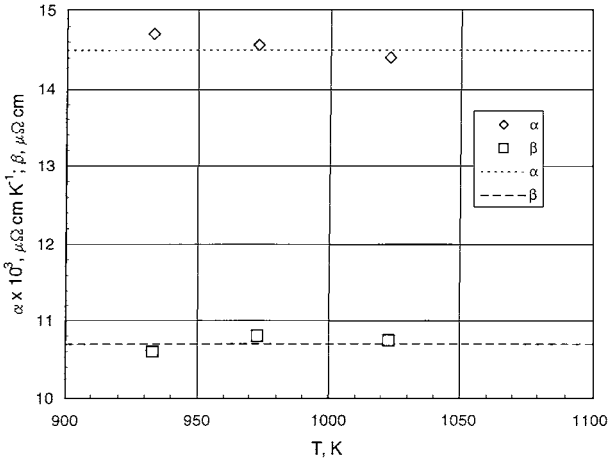

Figure 10 Variation of temperature coefficients of electrical resistivity against temperature for molten aluminum samples. Lines denote predicted values by Cusak and Enderby [22].

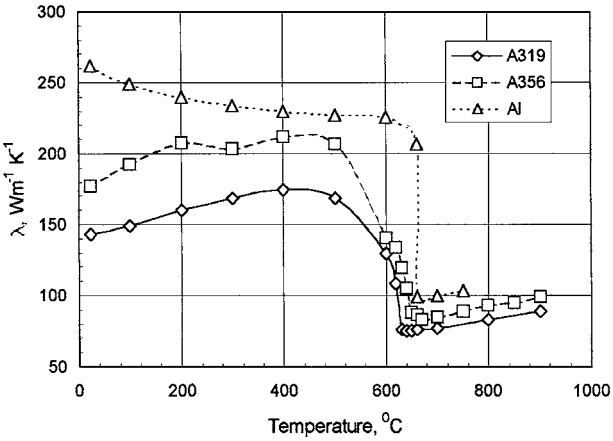

Figure 11 Variation of thermal conductivity with temperature for pure aluminum, A319 and A356 aluminum alloys.

where κ is the Boltzman constant, e is the electron charge. The constant

$$L_0 = \frac{\pi^2 \kappa^2}{3e^2} = 2.45 \times 10^{-8} W\,\Omega\,\mathrm{K}^{-2}$$

is the Lorenz number. The validity of this relationship was confirmed experimentally with high accuracy by many researchers [24–27]. The variation of the thermal conductivity estimated by the Wiedemann-Franz-Lorenz law against temperature is presented in Fig. 11.

4. Conclusions

A simple rotational technique to measure the electrical resistivity of molten metals has been developed and applied to pure aluminum, A319 and A356 aluminum alloys. The experimental method has been shown to exhibit eddy current damping consistent with theoretical predictions. Electrical resistivity data have been obtained for the test specimens over a wide range of temperatures. Excellent agreement has been found between experimental values from the present investigation and data from previous investigations for pure aluminum. The technique appears applicable to higher melting point metals and alloys.

Acknowledgments

The authors gratefully acknowledge the financial support received from the American Foundrymen's Society and NASA's Office of Life and Microgravity Sciences and Applications under Cooperative Agreement NCC8-128.

References

1. T. IIDA and R. I. L. GUTHRIE, "The Physical Properties of Liquid Metals," (Clarendon Press, Oxford, 1988) p. 227.
2. P. D. ADAMS and J. S. LEACH, *Physical Reviews* **156** (1967) 178.
3. Y. MERA, Y. KITA and A. ADACHI, *Technology Reports of Osaka University* **22** (1972) 445.
4. G. S. ERSHOV, A. A. KASATKIN and I. V. GAVRILIN, *Izv. Akad. Nauk SSSR. Metally* **2** (1976) 98.
5. H. K. MOFFATT, *J. Fluid Mechanics* **22**(3) (1965) 521.
6. W. BRAUNBECK, *Z. Phys*. **73** (1932) 312.
7. S. TAKEUCHI and H. ENDO, *Trans. Japan Inst. Metals* **3** (1962) 30.
8. K.-H. SPITZER, M. DUBKE and K. SCHWERDTFEGER, *Metallurgical Transactions B*, **17B** (1986) 119.
9. T. C. TOYE and E. E. JONES, *Proc. Phys. Soc*. **71** (1958) 88.
10. A. M. KOROLKOV and D. P. SHASHKOV, *Izv. Akad, Nauk. SSSR, Met. I Topl*. **1** (1962) 84.
11. A. ROLL and G. FEES, *Z. Metall*. **51** (1960) 540.
12. S. TAKEUCHI and H. ENDO, *J. Japan Inst. Metals* **26** (1962) 498.
13. *Idem*., *Trans. Japan Inst. Metals* **3** (1962) 35.
14. M. W. OZELTON and J. R. WILSON, *J. Sci. Instrum*. **43** (1996) 359.
15. A. M. SAMARIN, *Journal of The Iron and Steel Institute* **200** (1962) 95.
16. Y. ONO and T. YAGI, *Transactions of ISIJ* **12** (1972) 314.
17. L. D. LANDAU and E. M. LIFSHITZ, "Electrodynamics of Continuous Media," Ch. VII, (Pergamon Press, New York, 1960).
18. N. H. FRANK, Tech. Report. 23, MIT, Nov. 20, 1946.
19. L. HOLBORN, *Z. Phys*. **8** (1921) 58.
20. A. ROLL, H. FELGER and H. MOTZ, *Z. Metallkde*. **47** (1956) 707.
21. P. D. ADAMS, *PhD thesis*, University of London, 1964.
22. N. CUSACK and J. E. ENDERBY, *Proc. Phys. Soc*. **75** (1960) 395.
23. W.-K. RHIM and T. ISHIKAWA, *Review of Scientific Instruments* **69**(10) (1998) 3628.
24. G. BUSCH, H.-J. GÜNTHERODT and P. WYSSMANN, *Physics Letters* **39A** (1972) 89.
25. G. BUSCH, H.-J. GÜNTHERODT, W. HALLER and P. WYSSMANN, *ibid*. **41A** (1972) 29.
26. *Idem*., *ibid*. **43A** (1973) 225.
27. W. HALLER, H.-J. GÜNTHERODT and G. BUSCH, "Liquid Metals" (Inst. Phys. Conf. Ser. No. 30, 1976, 1977) p. 207.
28. S. I. BAKHTIYAROV and R. A. OVERFELT, *Journal of Materials Science* **34**(5) (1999) 945.
29. *Idem*., *Acta Materialia/Scripta Materialia* **47**(17) (1999) 4311.
30. Metal Casting R&D at Auburn University (http://metalcasting.auburn.edu/).

Received 19 September 2000
and accepted 6 June 2001